Design Simulations of MEMS Micropump by 3D Fluid-Structure Interaction Analysis

J. Johari* and B. Y. Majlis**

*Faculty of Electrical Engineering, Universiti Teknologi MARA
Selangor, Malaysia, julia893@salam.uitm.edu.my
**Institute of Microengineering and Nanoelectronics, IMEN
Universiti Kebangsaan Malaysia, Selangor, Malaysia, burhan@vlsi.eng.ukm.my

ABSTRACT

In this study, a three-way approach in designing a piezoelectrically actuated valveless micropump based on MEMS bulk micromachining fabrication process has been presented. The designed piezoelectrically actuated valveless micropump (PAVM) is analyzed using the fluid-structure interaction method to accurately predict the working behavior of the micropump based on the fluid, structural and piezoelectric equations. The fluid-structure dynamic effects should be taken into account in detail, since it is not enough to understand the intended functions individually due to the increasing demands for accuracy. In view of that, a coupled-field electro-mechanical-fluidic model of the PAVM has been simulated using MemFSI™, a fluid-structure interaction (FSI) solver available in CoventorWare™ software package. Results obtained from the simulations are compared with analytical studies for verification purposes.

Keywords: piezoelectrically actuated valveless micropump, fluid-structure interaction

1 INTRODUCTION

Micropumps are essential microfludics devices. The applications of such devices range from controlling and delivering tiny amounts of fluids from one point to another on a microfluidics system. Given the market potential for applications in microfluidics and drug delivery especially, micropumps are of considerable interest to researchers and industrial consumptions [1, 2]. Van de Pol and Van Lintel presented the first silicon micropump based on piezoelectric or thermopneumatic actuation of a thin membrane. Many micropumps have since been developed in the last few years based on different actuating principles and fabrication technologies. However, pump output characteristics and affecting factors have not been investigated thoroughly [3, 4].

Mechanical reciprocating displacement micropumps with vibrating membrane have generated the most interest among other type of micropumps. Even though various actuating principles of membrane micropumps have been developed such as piezoelectric, pneumatic, thermal, pneumatic, electrostatic, and electromagnetic, the piezoelectric type has been widely used. Because piezoelectrically actuated valveless micropump (PAVM) has simple structure and no internal moving parts, there is less risk of clogging the valves, when it pumps fluid containing particles. Also, they can respond quickly and have obvious advantages over other kinds of micropumps. See the review by Gong *et al* for more details [5].

Figure 1 shows the working principle of a PAVM, driven by a piezoelectric patch bonded to a diaphragm, which forces fluid through a small chamber.

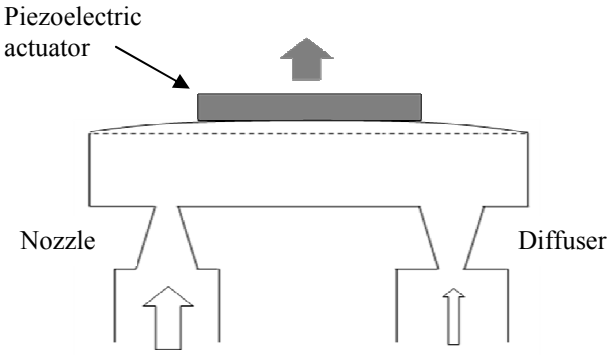

(a) Diaphragm bends up

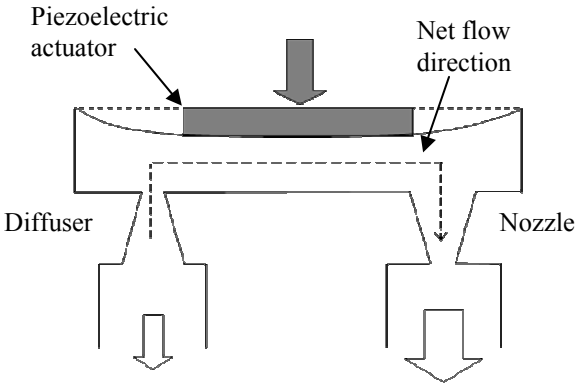

(b) Diaphragm bends down

Figure 1: The working principle of a PAVM.

In parallel flow, the flow rate through the diffuser is less than that through the diffuser because the resistance in the nozzle is higher than the resistance in the diffuser.

Therefore, when the diaphragm deflects upwards in the first half-cycle (figure 1(a)), more fluid will come into the chamber through the nozzle than through the diffuser. In other half cycle, the nozzle in the first half cycle acts as a diffuser when the diaphragm deflects downwards (figure 1 (b)), and less fluid goes through it. Hence there is net flow through in the complete cycle.

The characteristics of the PAVM have been researched since it was invented in 1990s. Li and Chen [6] show that there exists an optimal thickness, which depends on the thickness of the bonding layers by assuming a linear strain distribution across the thickness of the passive plate and the actuator. They found the optimal value for the ratio of passive plate thickness to diameter to be about 0.02. A comprehensive review of mathematical and numerical analysis of PZT actuator behaviour has been given by Chee *et al* [7].

On the fluids side, based on hydraulics theories, many researchers [10-14fromBFan] explained the working principle of the PAVM in their papers. They signified that the resistances across the diffuser and nozzle are different; therefore, the diffuser element can act as a passive valve and direct the net flow of the PAVM. Olsson [8] gave a simplified theoretical analysis of the pump flow and resonance frequency in 1995. Later, Olsson and Jiang [9, 10] investigated the diffuser flow at different Reynolds numbers and conical angles with commercial software and analytical methods. Nguyen showed that flow rate increases as the actuator membrane deflection increases and that the flow rate increases with increasing actuating frequencies at low frequency but remains almost constant when actuating frequencies approaches 60 Hz [11]. Gerlach's experiments [12, 13] demonstrated similar results that the pumping rate increases nearly linear at low frequencies and then reaches a maximum at an optimal actuating frequency; the pumping rate decreases sharply at higher frequencies.

Pan *et al* [14] used a perturbation method to study the fluid-membrane coupling analytically. Their analysis is based on the assumption that there is no pressure difference between the inlet and the outlet and they also assumed that the structural and geometric non-linearity could be neglected. The actuator is in fact a highly non-linear material and the pressure between the inlet and outlet is the only reacting force that the fluid applies on the membrane. Neglecting the pressure difference inside the chamber would lead to neglect of the membrane behaviour. Later, the same authors [15] show that the inertial force and the viscous loss of the fluid inside are of the same order of magnitude and neither can be neglected in the dynamic coupling analysis.

No complete coupling study has been conducted. This is the reason why some simulation results showed that flow rate increases continuously with the increase in frequency even at extremely high frequencies [16]. Complete coupling, especially the behaviour of the membrane and the deflection shape of the membrane at different frequencies, which may affect the pumping rate, needs to be studied.

In this paper, the finite element method and computational fluid dynamics are employed to study the fluid-membrane coupling and the membrane behaviour in a PAVM. This paper addresses how the actuating frequencies affect the performance of a PAVM.

2 GOVERNING EQUATIONS

A piezoelectric patch is utilized as the actuator. The special type, PZT is used in the simulation. Properties of PZT are given in table 1. The PZT density, ρ (kg m$^{-3)}$ is 7500 while the Poisson's ratio, λ is 0.3. The coupled electro-mechanical constitutive equation for the actuator is

$$\sigma_{ij} = C^{E}_{ijkl}\varepsilon_{kl} - e_{ijk}E_k \tag{1}$$

where ε_{kl} is the mechanical strain tensor, σ_{ij} is the mechanical stress tensor, E_k is the electric field vector, e_{ijk} is the piezoelectric constant tensor; C^{E}_{ijkl} is the elastic stiffness constant tensor at constant electric field.

Young's moduli ($\times 10^{11}$Pa)			Shear modulus ($\times 10^{11}$Pa)			Piezoelectric coefficients (C m^{-2})		
E_{31}	E_{33}	E_{15}	G_{31}	G_{33}	G_{15}	e_{31}	e_{33}	e_{15}
5.5	*6.2*	*6.2*	*2.33*	*2.3*	*2.3*	*-6.55*	*23.3*	*17*

Table 1: Properties of PZT

The silicon membrane in the PAVM is integrated with surrounding walls; therefore, it can be considered as a clamped plate. Properties of the silicon membrane are listed in table 2. The governing equation of forced vibration of thin clamped plate is

$$D\nabla^4 W + \rho_{s_i} h\frac{\partial^2 W}{\partial t^2} = f_e - P \tag{2}$$

where

$$D = \frac{Eh^3}{12\left(1-\nu^2\right)} \tag{3}$$

and f_e is the periodic actuating force, which can be solved from equation (1), E is the elastic modulus of the silicon membrane, ρ_{s_i} is the density of the silicon membrane, h is the thickness of the silicon membrane and P is the dynamic pressure exerted on the plate by the liquid. To

solve equation (2), P should be solved from the Navier-Stokes equations at every time step.

Property	Density, ρ	Young's moduli, E	Poisson's ratio, μ
Unit	kg m^{-3}	$\times 10^{11}$Pa	
Value	2330	1.62	0.22

Table 2: Silicon membrane properties

Since we assume the membrane to be clamped plate, displacements, curvatures and velocities of the clamped plate at edges should be zero. Therefore, the boundary conditions for a clamped plate can be written mathematically as

$$W = 0 \qquad x, y \in \partial\Omega \qquad (4)$$

$$\frac{\partial^2 W}{\partial x^2} = \frac{\partial^2 W}{\partial y^2} = 0 \qquad x, y \in \partial\Omega \qquad (5)$$

$$\frac{\partial W}{\partial t} = 0 \qquad x, y \in \partial\Omega \qquad (6)$$

Properties of the fluid used in this simulation are listed in table 3. Since the characteristics length of the micropump is of the order of 10^{-6} and the Reynolds number is very low, the flow can be considered as an incompressible laminar flow, which can be described using the Navier-Stoles equations (7).

$$\rho_L D\vec{V} / Dt = \rho_L \vec{g} + \mu \nabla^2 \vec{V} - \nabla P \qquad (7)$$

$$\frac{\partial \rho_L}{\partial t} + (\vec{V} \cdot \nabla)\rho_L = 0 \qquad (8)$$

Here, ρ_L is the density of the liquid; $\vec{V}$ is the velocity vector; μ is the viscosity of the liquid. Boundary conditions for fluid model are non-slip at fluid-wall interface and fluid-membrane interfaces and free surface boundary conditions at the inlet/outlet.

Property	Density, ρ_L	Dynamic viscosity, μ
Unit	kg m^{-3}	$\times 10^{-3}$ kg m^{-1}s^{-1}
Value	1000	1.4

Table 3: Fluid properties

3 SIMULATION OF ELECTRICAL-MECHANICAL-FLUIDIC COUPLING

The PZT actuator consists of a PZT patch and electrode layers on both sides. Because the electrode layers are very thin compared with the PZT patch, we can reasonably neglect electrode layers and just consider the model of the PZT, the silicon membrane and the fluid. In the design of the PAVM, the silicon membrane is centrally covered by a PZT patch and the PAVM chamber is fully covered by the PZT-silicon membrane bi-layer. The PZT patch has a thickness of 200 µm with length and width of 10 mm, and the silicon membrane is 100 µm thick with length and width of 12 mm. The PAVM chamber has a height 100 µm. The diffuser and nozzle have the same size; their throat width is 200 µm, height is 650 µm and included angle is 54.7°.

Meshing of the model for the micropump has been achieved using Manhattan bricks meshing for the diaphragm where increased density at the model edges has been used typically for fluidic simulations for the diffuser element to generate more accurate results as shown in figure 2. Mesh sensitivity analysis is conducted for all simulations to ensure that the simulation results will be independent of the meshing densities.

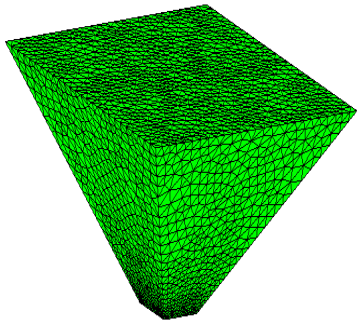

Figure 2: Diffuser element with increased meshing densities near the edges

The electro-mechanical behavior of the diaphragm has been simulated using CoSolve™ solver. Simulation to find the optimum aspect ratio of the diffuser element in order to obtain the highest diffuser efficiency has been performed using the MemCFD™ solver. Only laminar flow situations (Re = 200, 500 and 1000) are considered. Deviation of the pressure loss coefficient for the diffuser element between the diverging and converging direction is caused mainly by the pressure recovery characteristics of the flow during the diverging direction. To model the PZT actuator and the silicon diaphragm layer, a sinusoidal voltage is applied. The input voltage is connected at the top surface of PZT while the ground is at bottom surface of PZT. For the simulation to be accurate, grids at the centre area of each layer are denser than elsewhere.

4 SIMULATION RESULTS

Results of the PAVM analysis are presented in figure b4 and figure 5. The pumping rate is determined not only by the maximum deflection of the membrane and the fluid behaviour inside the chamber but also the deflection shape of the membrane. The deflection of the membrane is due to the shear stress applied on it by the actuator and the pressure of the fluid. This pressure is solved from Navier-Stokes equations by setting the deflection of the membrane as one of its boundary conditions. Therefore, the pumping behavior is a coupling of the fluid and the membrane.

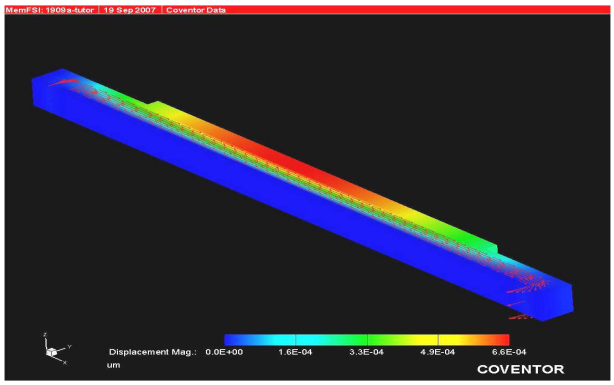

Figure 4: The 2D simulations showing the velocity profile of the fluid flow

Different actuating frequencies induce different deflection shapes; hence it affects the pumping rate. The pumping rate increases as the actuating frequency increases.

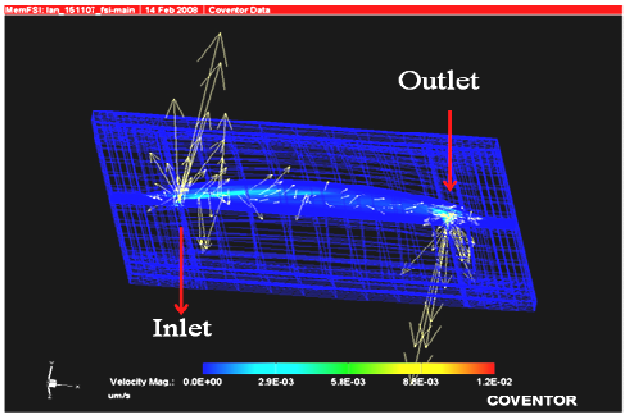

Figure 5: MemFSI™ simulation showing the velocity vector for fluid flow

5 CONCLUSIONS

This paper presents numerical studies of a piezoelectrically actuated valveless micropump with consideration of the three-way electro-mechanical-fluid couplings. Simulation results show that the pumping efficiency depends not only on the actuating frequencies and maximum magnitude of the membrane deflection, but also on the membrane deflection shape. At low actuating frequencies, the deflection shapes of the membrane are almost the same for various frequencies and the pumping rate is proportional to actuating frequency. The simulation indicates that the optimal actuating frequencies for the most efficient pumping rate should be less than the first natural frequency of the PZT bimorph at 29 kHz.

Simulation done in this work on a piezoelectric micropump can easily be adapted to various geometries and pump configurations, allowing analyzing the behavior of the flow in a wide range of microfluidic devices.

REFERENCES

[1] A. Nisar, N. Afzulpurkar, B. Mahaisavariya and A. Tuantranot, Sensors and Actuators, B 130, 917-942, 2008.

[2] F. Amirouche, Y. Zhou and T. Johnson, Microsystem Technology, Vol. 15, 647, 2009.

[3] H. T. G. Van Lintel, F. C. M. Van de Pol and S. Bouwstra, Sensors Actuators, A 15, 153-67, 1988.

[4] F. C. M. Van de Pol and H. T. G. Van Lintel, Sensors Actuators A, Phys. 21, 198-202, 1990.

[5] G. Song, B. Fan and F. Hussain, Proceedings of the 9th ASCE International Conference on Engineering, Constructions in Challenging Environments (Houston, TX), 664-671, 2004.

[6] S. Li and S. Chen, Sensors Actuators A 104, 151-61, 2003.

[7] C. Y. K Chee, L. Tong and G. P. Steven, J. Intell. Material System, 9, 3-19, 1998.

[8] A. Olsson, G. Stemme and E. Stemme, Sensors and Actuators A, Vol. 46-47, 549-556, 1995.

[9] A. Olsson, G. Stemme and E. Stemme, Sensors Actuators A, 84, 167-75, 2000.

[10] X. N. Jiang, Z. Y. Zhou, X. Y. Huang, Y. Li, Y. Yang and C.Y. Liu, Sensors Actuators A, 70, 81-87, 1998.

[11] N. T. Nguyen and X. Huang, Sensors Actuators A, 88, 104-111, 2001.

[12] T. Gerlach and H. Wurmus, Sensors Actuators A, 50, 135-40, 1995.

[13] T. Gerlach, M. Schuenemann and H. Wurmus, J. Micromech. Microeng., 5, 199-201, 1995.

[14] L. S. Pan, T. Y. Ng, G. R. Liu, K. Y. Lam and T. Y. Jiang, Sensors Actuators A, 93, 173-81, 2001.

[15] L. S. Pan, T. Y. Ng, X. H. Wu and H. Lee, J. Micromech. Microeng., 13, 390-9, 2003.

[16] C. G. J. Schabmueller, M. Koch, M. E. Mokhtari, A. G. R. Evans, A. Brunnschweiler and H. Sehr, J. Micromech. Microeng., 12, 420-4, 2002.